

Synthesis and solution fluxionality of rhenium(i) carbonyl complexes of 2,4,6-tris(pyrazol-1-yl)-1,3,5-triazines (L), [ReX(CO)₃L] (X = Cl, Br or I). Characterization of [{ReX(CO)₃}₂L] (X = Cl or Br)

Andrew Gelling, Keith G. Orrell, Anthony G. Osborne and Vladimir Šik

Department of Chemistry, The University, Exeter EX4 4QD, UK

The stable octahedral complexes *fac*-[ReX(CO)₃L] [X = Cl, Br or I; L = 2,4,6-tris(4-methylpyrazol-1-yl)-1,3,5-triazine (tmpzt) or 2,4,6-tris(3,5-dimethylpyrazol-1-yl)-1,3,5-triazine (tdmpzt)] have been prepared in which the substituted triazines act as bidentate chelate ligands. In solution the complexes are fluxional with the nitrogen ligand oscillating between two equivalent bonding modes. Rates and activation energies for the fluxion have been investigated by dynamic NMR methods. Activation energies ΔG^\ddagger (298.15 K) are in the range 47–72 kJ mol⁻¹ and are dependent on the steric requirements of the pyrazole groups. At low temperatures changes in the ¹H NMR spectra are interpreted in terms of varying rates of rotation of one of the unco-ordinated pyrazole rings. The non-fluxional dimetallic complexes [{ReX(CO)₃}₂L] (X = Cl or Br; L = tdmpzt) were also isolated and structurally characterized by ¹H NMR spectroscopy.

In a series of papers ^{1–4} we have reported studies on some metal complexes of potentially terdentate ligands such as 2,2':6',2'' terpyridine (terpy) or 2,6-bis(pyrazol-1-yl)pyridine (bppy) where the ligands are acting in a bidentate chelate mode towards kinetically inert metal moieties such as *fac*-ReX(CO)₃ or *fac*-PtXMe₃. Such complexes were found to undergo a 1,4-metallotropic shift in solution whereby the three donor nitrogen atoms of the ligand become involved with the metal. Our studies have mainly involved systems with one metal centre and terdentate ligands that can be considered as being derived from a central heterocyclic ring with two peripheral heterocyclic rings. We now wish to extend our studies to other ligands that could accommodate more than one metal centre. Such ligands can be considered to be built up from a central heterocyclic ring *e.g.* 1,3-pyrimidine or 1,3,5-triazine and three peripheral rings such as pyrazol-1-yl or 2-pyridyl. We have recently reported ⁵ results for some rhenium complexes of pyrazolylpyrimidine ligands. We now report some studies on rhenium complexes of the pyrazolyltriazines 2,4,6-tris(4-methylpyrazol-1-yl)-1,3,5-triazine (tmpzt) and 2,4,6-tris(3,5-dimethylpyrazol-1-yl)-1,3,5-triazine (tdmpzt). Such compounds can in principle form complexes by acting in a bidentate bonding mode to up to three metals, in a terdentate mode to one or two metals, or in a combination of ter- and bi-dentate modes. We describe here solution NMR studies of the 1:1 metal:ligand complexes *fac*-[ReX(CO)₃L] (X = Cl, Br or I; L = tmpzt or tdmpzt) and on the 2:1 complexes [{ReX(CO)₃}₂(tdmpzt)] (X = Cl or Br).

Experimental

Materials

The complexes [ReX(CO)₃] (X = Cl, Br or I) were prepared using previously described methods.^{6,7} 4-Methylpyrazole was obtained from Acros Chimica and used without further purification. 3,5-Dimethylpyrazole and 2,4,6-trichloro-1,3,5-triazine were obtained from Aldrich Chemicals and used without further purification.

Synthesis of tris(pyrazolyl)triazines

2,4,6-Tris(4-methylpyrazol-1-yl)- and 2,4,6-tris(3,5-dimethylpyrazol-1-yl)-1,3,5-triazine were prepared in an analogous manner from the addition of 2,4,6-trichloro-1,3,5-triazine

to the potassium salt of the corresponding pyrazole. The preparation of 2,4,6-tris(4-methylpyrazol-1-yl)-1,3,5-triazine is described below.

2,4,6-Tris(4-methylpyrazol-1-yl)-1,3,5-triazine. 2,4,6-Trichloro-1,3,5-triazine (1.12 g, 6.07 mmol) was added to 3 molar equivalents of potassium 4-methylpyrazolate [prepared from equimolar quantities of 4-methylpyrazole and potassium metal at 70 °C in anhydrous diglyme (2,5,8-trioxanonane) (15 cm³)] and the resultant mixture was stirred at room temperature for 3 h. The yellow suspension was then added to water (150 cm³) and the mixture stirred in an ice-bath for 1 h to yield a white precipitate. The precipitate was isolated, dissolved in dichloromethane (20 cm³), dried (MgSO₄) and the solvent removed *in vacuo* to give a white oily solid which was washed with light petroleum (b.p. 40–60 °C) (100 cm³) to yield the desired product as a white powder (0.54 g) in 28% yield.

Synthesis of complexes

All preparations were carried out using standard Schlenk techniques⁸ under purified nitrogen using freshly distilled and degassed solvents.

1:1 Complexes. The complexes [ReX(CO)₃L] (L = tmpzt and tdmpzt; X = Cl, Br or I) were all prepared in a similar manner. The details for [ReBr(CO)₃(tdmpzt)] are given below. Synthetic, analytical and mass spectral data are listed in Tables 1 and 2.

Bromotricarbonyl[2,4,6-tris(3,5-dimethylpyrazol-1-yl)-1,3,5-triazine]rhenium(i). The compound [ReBr(CO)₃] (0.22 g, 0.54 mmol) and tdmpzt (0.2 g, 0.55 mmol) were dissolved in benzene (50 cm³) and the mixture heated under reflux for 4 h, after which time its solution infrared spectrum showed loss of signals (at 2155, 2047 and 1987 cm⁻¹) attributable to [ReBr(CO)₃]. The volume was reduced to \approx 15 cm³ and light petroleum (120 cm³) added to precipitate a yellow solid. The almost colourless solvent was decanted and the solid was dried under vacuum. Recrystallization from dichloromethane–hexane gave the desired product as yellow crystals. Yield 0.31 g (80%).

2:1 Complexes. The complexes [{ReX(CO)₃}₂(tdmpzt)] (X = Cl or Br) were both prepared in a similar manner. The synthesis was analogous to that for the 1:1 complexes, but with

a 2:1 ratio of metal reactant to ligand. The solution was refluxed for ≈ 24 h and worked up as for the 1:1 complex to yield the desired product as an orange precipitate in 20–24% yield.

Physical methods

Hydrogen-1 NMR spectra were recorded on either a Bruker AC-300 or DRX-400 spectrometer operating at 300.13 or 400.13 MHz respectively in CDCl_3 , CD_2Cl_2 or $\text{CDCl}_2\text{CDCl}_2$ solutions. A standard B-VT 1000 variable-temperature unit was used to control the probe temperature, the calibration of this unit being checked periodically against a Comark digital thermometer. The temperatures are considered accurate to $\pm 1^\circ\text{C}$. Two-dimensional exchange (EXSY) NMR spectra of the complex $[\text{ReBr}(\text{CO})_3(\text{tmpzt})]$ using the Bruker NOESYPH program were recorded with mixing times of 0.2–2.0 s. Signal intensities were obtained by accurate row integration. Rate data, for the $[\text{ReX}(\text{CO})_3(\text{tdmpzt})]$ complexes, were based on bandshape analysis of ^1H NMR spectra using the authors'

version of the standard DNMR 3 program.⁹ Activation parameters based on experimental rate data were calculated using the THERMO program.¹⁰ Rate data for the $[\text{ReX}(\text{CO})_3(\text{tmpzt})]$ complexes were calculated from intensity data using our D2DNMR program.¹¹

Infrared spectra were recorded on a Perkin-Elmer 881 spectrometer calibrated from the signal of polystyrene at 1602 cm^{-1} , electron-impact mass spectra on a Kratos Profile spectrometer. Elemental analyses were performed by Butterworth Laboratories, Teddington, Middlesex, London.

Results

The air-stable complexes were characterized by elemental analysis, IR and mass spectral data (Tables 1 and 2). The three strong IR absorptions confirm the expected facial disposition of the three carbonyl groups in the complexes. The NMR data for free tmpzt and tdmpzt in CDCl_3 are given in Table 3. The high symmetries of the molecules lead to simple ^1H spectra which are readily analysed. All scalar couplings are approximately zero

Table 1 Synthetic and analytical data for the complexes $[\text{ReX}(\text{CO})_3\text{L}]$ ($\text{X} = \text{Cl, Br or I}$; $\text{L} = \text{tmpzt or tdmpzt}$) and $[\{\text{ReX}(\text{CO})_3\}_2(\text{tdmpzt})]$ ($\text{X} = \text{Cl or Br}$)

Complex	Yield ^a (%)	$\tilde{\nu}_{\text{CO}}$ ^b / cm^{-1}	Analysis ^c (%)		
			C	H	N
$[\text{ReCl}(\text{CO})_3(\text{tmpzt})]$	36	2030s, 1926s, 1900s	33.9 (34.45)	2.90 (2.40)	16.55 (20.1)
$[\text{ReBr}(\text{CO})_3(\text{tmpzt})]$	68	2031s, 1927s, 1901s	33.4 (32.2)	2.10 (2.20)	17.8 (18.8)
$[\text{ReI}(\text{CO})_3(\text{tmpzt})]$	45	2030s, 1928s, 1904s	31.2 (30.1)	2.30 (2.10)	16.25 (17.55)
$[\text{ReCl}(\text{CO})_3(\text{tdmpzt})]$	73	2028s, 1925s, 1900s	37.2 (37.7)	2.95 (3.15)	17.55 (18.85)
$[\text{ReBr}(\text{CO})_3(\text{tdmpzt})]$	80	2029s, 1929s, 1902s	35.4 (35.3)	2.70 (2.95)	17.3 (17.7)
$[\text{ReI}(\text{CO})_3(\text{tdmpzt})]$	76	2028s, 1929s, 1904s	32.7 (33.2)	2.60 (2.80)	15.8 (16.6)
$[\{\text{ReCl}(\text{CO})_3\}_2(\text{tdmpzt})]$	24	2031s, 1920s, 1899s	29.7 (29.6)	2.25 (2.15)	12.85 (12.95)
$[\{\text{ReBr}(\text{CO})_3\}_2(\text{tdmpzt})]$	20	2029s, 1922s, 1902s	27.15 (27.1)	2.00 (2.00)	10.85 (11.9)

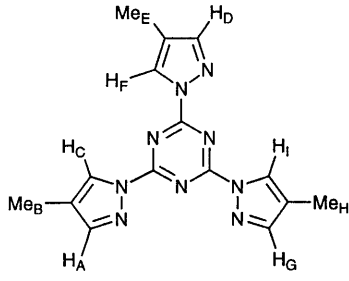
^a Relative to metal-containing reactant. ^b Recorded in benzene; s = strong. ^c Calculated values in parentheses.

Table 2 Mass spectral data for the complexes $[\text{ReX}(\text{CO})_3\text{L}]$ ($\text{X} = \text{Cl, Br or I}$; $\text{L} = \text{tmpzt or tdmpzt}$)

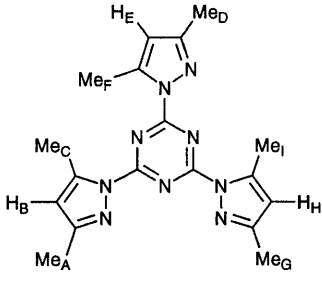
Complex	m/z					
	$[M]^+$	$[M - \text{CO}]^+$	$[M - 2\text{CO}]^+$	$[M - 3\text{CO}]^+$	$[M - 3\text{CO} - \text{X}]^+$	$[L]^+$
$[\text{ReCl}(\text{CO})_3(\text{tmpzt})]$	—	—	—	—	507	321
$[\text{ReBr}(\text{CO})_3(\text{tmpzt})]$	—	—	—	—	507	321
$[\text{ReI}(\text{CO})_3(\text{tmpzt})]$	719	691	663	635*	508	321
$[\text{ReCl}(\text{CO})_3(\text{tdmpzt})]$	669	641*	613	585	—	363
$[\text{ReBr}(\text{CO})_3(\text{tdmpzt})]$	714	686*	658	630	550*	363
$[\text{ReI}(\text{CO})_3(\text{tdmpzt})]$	761	733*	705	677	550*	363

* Most abundant peak.

Table 3 Hydrogen-1 NMR data* for the tris(pyrazol-1-yl)triazines in CDCl_3 at 303 K



tmpzt



tdmpzt

δ

Compound	H _A	H _B	H _C	H _D	H _E	H _F	H _G	H _H	H _I
tmpzt	7.65	2.07	8.41	7.65	2.07	8.41	7.65	2.07	8.41
tdmpzt	2.09	5.87	2.59	2.09	5.87	2.59	2.09	5.87	2.59

* Chemical shifts, δ , relative to SiMe_4 (δ 0); spin-spin coupling constants *ca.* 0 except for $^4J(\text{H}_B\text{H}_C)$, $^4J(\text{H}_E\text{H}_F)$ and $^4J(\text{H}_H\text{H}_I)$ which have a magnitude of 0.75 Hz.

with the exception of those between the 4-position methyl and 5-position methine hydrogens [*viz.* $^4J(\text{H}_\text{B}\text{H}_\text{C})$, $^4J(\text{H}_\text{E}\text{H}_\text{F})$ and $^4J(\text{H}_\text{H}\text{H}_\text{I})$] which have a magnitude of 0.75 Hz.

[ReX(CO)₃(tdmpzt)] complexes

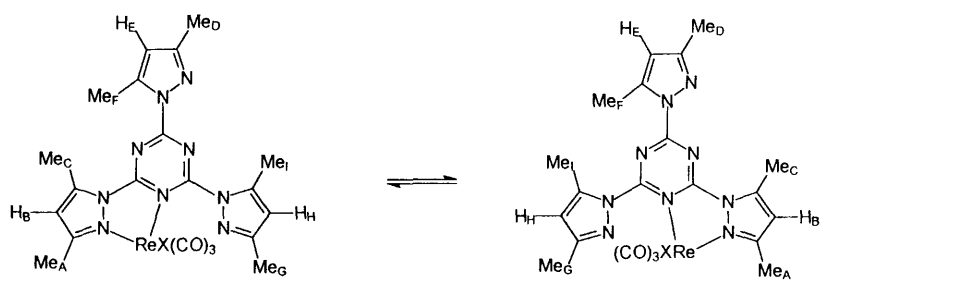
Chemical shift data for the three halide complexes [ReX(CO)₃(tdmpzt)] are collected in Table 4. Co-ordination shifts, $\Delta\delta$, are also given, but only *relative* magnitudes of such shifts should be noted as they refer to spectra of free pro-ligands and complexes recorded in different solvents and at somewhat different temperatures.

Variable-temperature ^1H NMR spectra of the three tdmpzt complexes were recorded in the approximate range 273–393 K. On raising the solution temperatures of these complexes exchanges occurred between the pyrazolyl-ring hydrogen signals B and H, and between the methyl hydrogen signals A and G, and between C and I, as expected for a 1,4-metallotropic shift as depicted at the head of Table 4. Signal coalescences occurred at *ca.* 323 K for the B \rightleftharpoons H system and at *ca.* 333 K for the A \rightleftharpoons G and C \rightleftharpoons I systems. The signals associated

with the third pyrazolyl ring, which is not involved in the metal co-ordination, remain sharp throughout this temperature range. Bandshape analyses were carried out on the B \rightleftharpoons H spin problem as this was judged to be the most sensitive to the fluxional process. For each halide complex approximately ten experimental spectra, recorded in the range 283–383 K, were fitted and activation-energy data calculated.

On cooling CD_2Cl_2 solutions of these complexes below 273 K further changes were noted in certain of the methyl signals, mainly methyls C, F and I. These signals became increasingly broad on cooling and eventually split into slightly unequal-intensity pairs at temperatures below *ca.* 200 K (Table 5). This was attributed to a slowing down of the rotation of the pyrazolyl ring adjacent to the ReX(CO)₃ moiety. Justification of this assumption is borne out by the detailed interpretation of the spectra of the tpmpt complexes (next section). The other unco-ordinated pyrazolyl ring remote from the rhenium moiety appears to rotate rapidly on the NMR time-scale at all accessible temperatures. The changing bandshapes of the signals due to methyls C and L were recorded and an estimate made of the rate of the ring-rotation process at the coalescence

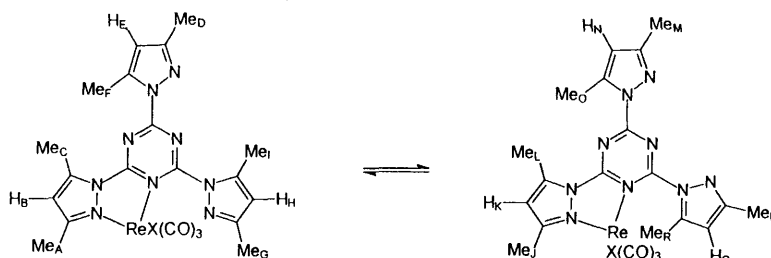
Table 4 Hydrogen-1 NMR data * for the complexes [ReX(CO)₃(tdmpzt)] at temperatures where the metallotropic shift is slow



X	Solvent	T/K	H _A	H _B	H _C	H _D	H _E	H _F	H _G	H _H	H _I
Cl	CD ₂ Cl ₂	233	2.56 (0.47)	6.34 (0.47)	2.83 (0.24)	2.28 (0.19)	6.21 (0.34)	2.67 (0.08)	2.29 (0.20)	6.23 (0.36)	2.63 (0.04)
Br	CDCl ₂ CDCl ₂	253	2.55 (0.46)	6.30 (0.43)	2.83 (0.24)	2.29 (0.20)	6.19 (0.32)	2.63 (0.04)	2.31 (0.22)	6.21 (0.34)	2.60 (0.01)
I	CD ₂ Cl ₂	243	2.55 (0.46)	6.37 (0.50)	2.88 (0.29)	2.29 (0.20)	6.22 (0.35)	2.66 (0.07)	2.30 (0.21)	6.22 (0.35)	2.59 (0.00)

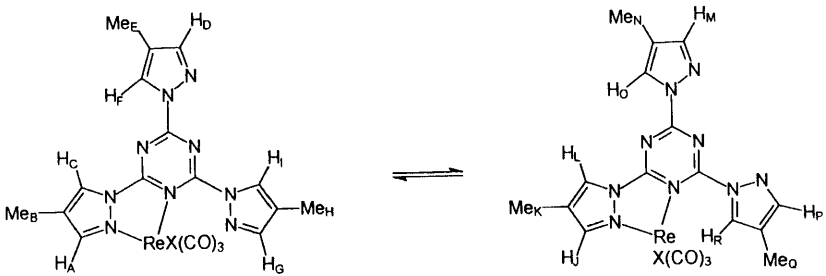
* Chemical shifts, δ , relative to SiMe₄ (δ 0); co-ordination shifts, $\Delta\delta$, in parentheses.

Table 5 Hydrogen-1 NMR data * for the pairs of conformers of the complexes [ReX(CO)₃(tdmpzt)] in CD₂Cl₂ at 178 K



X	H _A /H _J	H _B /H _K	H _C /H _L	H _D /H _M	H _E /H _N	H _F /H _O	H _G /H _P	H _H /H _Q	H _I /H _R
Cl	2.53 (H _A) ≈ 2.53 (H _J) (≈ 0)	6.34 (H _B) ≈ 6.34 (H _K) (≈ 0)	2.81 (H _C) 2.73 (H _L) (0.08)	2.26 (H _D) 2.24 (H _M) (0.02)	6.21 (H _E) ≈ 6.21 (H _N) (≈ 0)	2.62 (H _F) 2.68 (H _O) (−0.06)	2.27 (H _G) ≈ 2.27 (H _P) (≈ 0)	6.23 (H _H) ≈ 6.23 (H _Q) (≈ 0)	2.57 (H _I) 2.62 (H _R) (−0.05)
Br	2.51 (H _A) 2.52 (H _J) (−0.01)	6.34 (H _B) ≈ 6.34 (H _K) (≈ 0)	2.81 (H _C) 2.73 (H _L) (0.08)	2.25 (H _D) 2.23 (H _M) (0.02)	6.21 (H _E) ≈ 6.21 (H _N) (≈ 0)	2.61 (H _F) 2.67 (H _O) (−0.06)	2.27 (H _G) 2.28 (H _P) (−0.01)	6.23 (H _H) ≈ 6.23 (H _Q) (≈ 0)	2.55 (H _I) 2.60 (H _R) (−0.05)
I	2.50 (H _A) 2.51 (H _J) (−0.01)	6.36 (H _B) ≈ 6.36 (H _K) (≈ 0)	2.83 (H _C) 2.75 (H _L) (0.08)	2.25 (H _D) 2.23 (H _M) (0.02)	6.22 (H _E) ≈ 6.22 (H _N) (≈ 0)	2.61 (H _F) 2.67 (H _O) (−0.06)	2.28 (H _G) 2.27 (H _P) (0.01)	6.24 (H _H) ≈ 6.20 (H _Q) (≈ 0.04)	2.54 (H _I) 2.58 (H _R) (−0.04)

* Chemical shifts, δ , relative to SiMe₄ (δ 0); rotamer chemical shift differences, $\Delta\delta$, in parentheses.

Table 6 Hydrogen-1 NMR data * for the pairs of static structures of the complexes $[\text{ReX}(\text{CO})_3(\text{tmpzt})]$ in CD_2Cl_2


X	T/K	δ	$\text{H}_\text{A}/\text{H}_\text{J}$	$\text{H}_\text{B}/\text{H}_\text{K}$	$\text{H}_\text{C}/\text{H}_\text{L}$	$\text{H}_\text{D}/\text{H}_\text{M}$	$\text{H}_\text{E}/\text{H}_\text{N}$	$\text{H}_\text{F}/\text{H}_\text{O}$	$\text{H}_\text{G}/\text{H}_\text{P}$	$\text{H}_\text{H}/\text{H}_\text{Q}$	$\text{H}_\text{I}/\text{H}_\text{R}$
Cl	213		8.10 (H_A) 8.10 (H_J) (0.0)	2.21 (H_B) 2.22 (H_K) (-0.01)	8.50 (H_C) 8.56 (H_L) (-0.06)	7.83 (H_D) 7.83 (H_M) (0.0)	2.14 (H_E) 2.15 (H_N) (-0.01)	8.37 (H_F) 8.37 (H_O) (0.0)	7.89 (H_G) 7.88 (H_P) (0.01)	2.19 (H_H) 2.18 (H_Q) (0.01)	8.31 (H_I) 8.30 (H_R) (0.01)
Br	198		8.10 (H_A) 8.14 (H_J) (-0.04)	2.19 (H_B) 2.22 (H_K) (-0.03)	8.49 (H_C) 8.56 (H_L) (-0.07)	7.83 (H_D) 7.83 (H_M) (0.0)	2.15 (H_E) 2.15 (H_N) (0.0)	8.35 (H_F) 8.35 (H_O) (0.0)	7.89 (H_G) 7.88 (H_P) (0.01)	2.18 (H_H) 2.15 (H_Q) (0.03)	8.32 (H_I) 8.30 (H_R) (0.02)
I	198		8.12 (H_A) 8.13 (H_J) (-0.01)	2.20 (H_B) ? ?	8.52 (H_C) 8.54 (H_L) (-0.02)	7.84 (H_D) 7.83 (H_M) (0.01)	2.13 (H_E) 2.13 (H_N) (0.0)	8.36 (H_F) 8.36 (H_O) (0.0)	7.90 (H_G) 7.88 (H_P) (0.02)	2.17 (H_H) ≈ 2.13 (H_Q) (≈ 0.04)	8.29 (H_I) 8.27 (H_R) (0.02)

* Chemical shifts, δ , relative to SiMe_4 (δ 0); rotamer chemical shift difference, $\Delta\delta$, in parentheses.

temperature of the bands. Similar spectral changes were recorded for all three halide complexes and activation energies were calculated as above.

$[\text{ReX}(\text{CO})_3(\text{tmpzt})]$ complexes

The room-temperature ^1H NMR spectra of these complexes consist of six signals which comprise four ring methine signals (relative intensity 2:2:1:1) and two ring methyl signals (relative intensity 6:3). These are fully consistent with six-coordinate rhenium(i) complexes in which the metal moiety is undergoing rapid exchange between equivalent, bidentate, chelate forms, and in which both unco-ordinated pyrazolyl rings are rapidly rotating about the N-C bonds connecting them to the central triazine ring. On cooling the solutions of these complexes the spectra show extensive and complex changes. All signals associated with the two pyrazolyl rings involved in metal co-ordination broaden, then split, and eventually sharpen until at ca. 200 K ten methine signals (two of which are overlapping pairs) and six methyl signals are detected. These may be interpreted as due to the slowing down of both the 1,4-metallotropic shift and rotation of the unco-ordinated pyrazolyl ring adjacent to the rhenium moiety, such that at the limiting low temperatures the signals may be attributed to the two static species shown at the head of Table 6.

It is clear that in these tmpzt complexes the fluxional shifts and restricted pyrazolyl-ring rotations occur at comparable rates, and so their individual measurement requires more detailed consideration. The full dynamic problem is represented by Fig. 1. It is likely (see below) that the unco-ordinated pyrazolyl ring adjacent to the metal centre preferentially adopts near-orthogonal conformations with respect to the central triazine ring. There are two such conformations, *viz.* structures **a** or **b** and **c** or **d** (Fig. 1). Both pyrazolyl rings involved in the metal co-ordination must necessarily undergo some rotations in order to accommodate the 1,4-metal shifts. One metal fluxion pathway [(i) in Fig. 1] can involve near-90° clockwise rotations of the pyrazolyl rings, one rotation being prior to, and the other rotation subsequent to, the metal fluxion. A second pathway [(ii) in Fig. 1], which exchanges structures **c** and **d**, is totally analogous to (i) but involves near-90° anticlockwise (or near-270° clockwise) rotations. The other fluxion pathways [(iii) in Fig. 1] involve a combination of near-90°

clockwise and near-90° anticlockwise rotations of the pairs of pyrazolyl rings. The two remaining pathways [(iv) in Fig. 1] involve pure 180° rotations of the unco-ordinated pyrazolyl ring.

In order to investigate the relative rates of these exchange pathways two-dimensional EXSY spectra of the methine hydrogens were recorded at temperatures just below the onset of exchange broadening, *viz.* ca. 210 to 190 K. The ^1H spectrum of $[\text{ReBr}(\text{CO})_3(\text{tmpzt})]$ at 208 K is shown as a typical example (Fig. 2). Cross-peaks are detected between signals L and C and between G and P, indicative of slow rotation of the pyrazolyl ring *via* pathways (iv). Cross-peaks detected between the signal pairs L, I and C, R provide evidence for the fluxion plus rotation pathways (iii). The *absence* of any cross-peaks between L and R and between C and I suggest that pathways (i) and (ii) involving two clockwise or anticlockwise rotations of the pyrazolyl rings are *not* favoured. Additional cross-peaks between the partially resolved signal pairs A/J and G/P may be ascribed to the exchanges $\text{J} \rightleftharpoons \text{G}$ and $\text{A} \rightleftharpoons \text{P}$, *i.e.* *via* pathways (iii). Thus, the two-dimensional spectrum provides clear evidence for restricted pyrazolyl ring rotation and 1,4-Re-N shifts which are accompanied by rotations of the two involved pyrazolyl rings, these rotations being in opposite senses. These findings were quantified by analysing the diagonal and cross-peak signal intensities of the two-dimensional EXSY spectra using the authors D2DNMR program.¹¹

The region including the diagonal and cross-peak signals of methine hydrogens L, C, I or R was chosen for the rate calculations. Relative intensities of the four diagonal and six off-diagonal signals were measured accurately by row integration of the spectral matrix. The population matrix *P* for the four methine environments was calculated from the relative populations of the four structures (Fig. 1), these being 22.5 (**a**), 22.5 (**b**), 27.5 (**c**) and 27.5% (**d**). Rate constants for the fluxion-plus-rotation process [pathways (iii)] and the pyrazolyl-ring rotation [pathways (iv)] were extracted as the appropriate off-diagonal elements of the computed kinetic matrix, *L*.¹¹ Values are given in Table 7 and are based on an optimized mixing time of 0.3 s for the NOESY pulse sequence. This procedure was then repeated for two-dimensional EXSY spectra recorded at 203, 198 and 193 K, with the mixing times being increased proportionately to allow for the slower rates of magnetization transfer as the temperature is lowered. The four pairs of rate

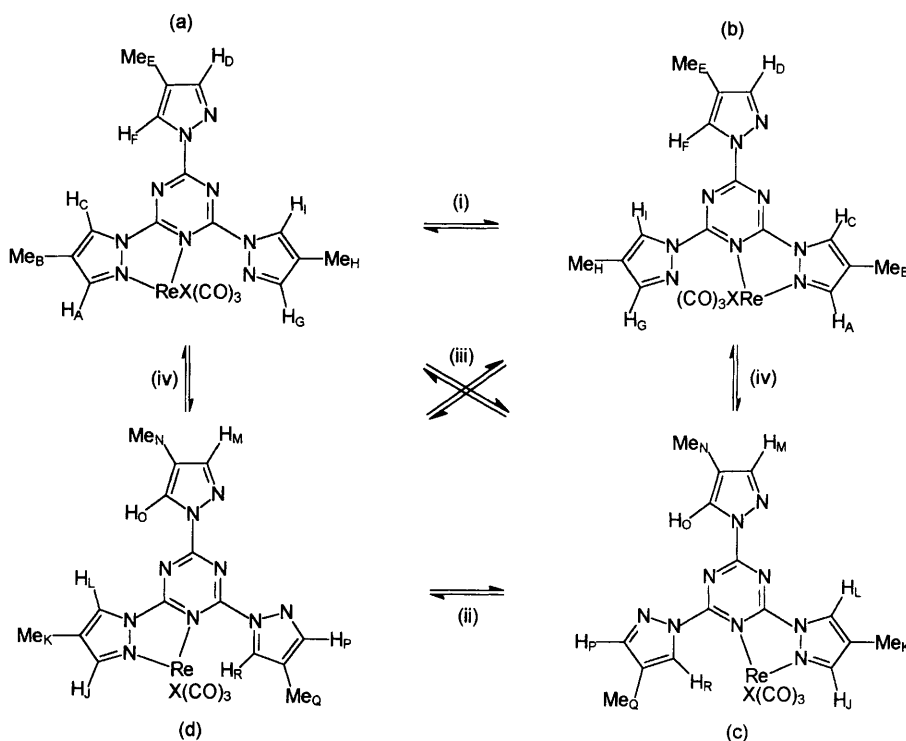


Fig. 1 Exchange pathways associated with the 1,4-metallotropic shifts and 4-methylpyrazolyl ring rotations in the complexes $[\text{ReX}(\text{CO})_3(\text{tmpzt})]$. See text for description of pathways (i)–(iv)

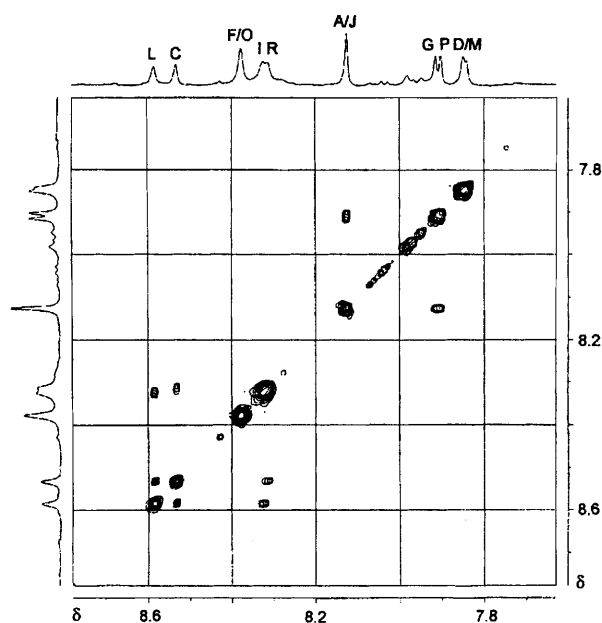


Fig. 2 Hydrogen-1 400 MHz two-dimensional EXSY NMR spectrum of $[\text{ReBr}(\text{CO})_3(\text{tmpzt})]$ at 208 K; mixing time 0.3 s. See Fig. 1 for signal labelling

constants (Table 7) gave good linear Eyring plots with temperature which enabled exchange rates to be reliably predicted for the higher-temperature region where exchange-broadened spectra were detected. In order to provide further support to the reliability of the EXSY-derived rate data, spectra in the range 203–288 K were fitted by bandshape analysis using these extrapolated rate values (Table 7). Very satisfactory fits were achieved between the experimental and computer-simulated spectra as depicted in Fig. 3. In these spectra it should be noted that only the bandshapes of hydrogens L, C, I and R were fitted, the composite signal due to hydrogens F and O on the third pyrazolyl ring being virtually temperature independ-

Table 7 Kinetic data^a for the fluxions of $[\text{ReBr}(\text{CO})_3(\text{tmpzt})]$

<i>T</i> /K	Mixing time ^b /s	<i>k</i> ₁ ^c /s ^{−1}	<i>k</i> ₂ ^d /s ^{−1}
193	2.0	0.08	0.06
198	1.5	0.19	0.14
203	1.0	0.42	0.30
208	0.3	0.84	0.65
213	—	1.76	1.28
223	—	6.44	4.81
233	—	21.8	16.1
253	—	176.8	130.3
263	—	462.9	335.3
268	—	735.1	523.2
278	—	1690	1200
288	—	3687	2618

^a At temperatures 193–208 K, derived from two-dimensional EXSY spectra. Higher-temperature values are based on Eyring-plot extrapolations. ^b Optimized values to give greatest accuracy of rate data. ^c For fluxion + rotation process, pathways (iii), Fig. 1. ^d For pyrazolyl-ring rotation, pathways (iv), Fig. 1.

ent. Further at temperatures above *ca.* 223 K a weak decomposition band at δ 8.43 is present which at higher temperatures overlaps with the coalesced signal of the methine hydrogens L, C, I and R.

For the complex $[\text{ReCl}(\text{CO})_3(\text{tmpzt})]$ analogous rate data were obtained from two-dimensional EXSY spectra recorded in the range 198–218 K; for $[\text{ReI}(\text{CO})_3(\text{tmpzt})]$ such spectra were obtained in the range 198–213 K.

$[\{\text{ReX}(\text{CO})_3\}_2(\text{tdmpzt})]$ (X = Cl or Br)

These 2:1 metal:ligand complexes were synthesized and their NMR chemical shift data are given in Table 8. The presence of two methine signals (relative intensity 2:1) and four methyl signals (6:6:3:3) is consistent either with the symmetrical 2:1 complex (structure **f**, Table 8) or with rapid exchange of this structure with the two equivalent structures **e** and **g** arising from

1,4-metallotropic shifts of either $\text{ReX}(\text{CO})_3$ moiety. Variable-temperature NMR studies of both these halide complexes failed to reveal any significant changes in the methine and methyl signals, suggesting that they exist solely as the symmetrical structure **f** which possesses an effective plane of symmetry

through the C–N bond linking the unco-ordinated pyrazolyl ring to the triazine ring. [View Article Online](#)

Discussion

Activation-energy data for the two distinct intramolecular dynamic processes of the $[\text{ReX}(\text{CO})_3(\text{tmpzt})]$ and $[\text{ReX}(\text{CO})_3(\text{tdmpzt})]$ complexes are collected in Table 9. In the case of the tdmpzt complexes the rates of rotation of the unco-ordinated pyrazolyl ring are always considerably greater than those of the 1,4-Re–N fluxion so that their influences on the spectral line shapes cover different temperatures ranges. The two processes could therefore be quantified independently. By contrast, in the case of the tmpzt complexes, the fluxion and rotation processes proceed at very similar rates and are thus strongly correlated. This allows greater insight into their likely mechanisms. The preferred static conformations of these complexes are assumed to involve the unco-ordinated pyrazolyl ring adjacent to the metal centre to be considerably oriented with respect to the plane of the central triazine ring. This is in accord with the crystal structures of the closely related complexes $[\text{ReBr}(\text{CO})_3\text{L}]$ [$\text{L} = 6\text{-(pyrazol-1-yl)-2,2'}$ -bipyridine (pbipy) or $6\text{-(3,5-dimethylpyrazol-1-yl)-2,2'}$ -bipyridine (dmpbipy)].⁴ In these previous cases the rotation of the unco-ordinated pyrazolyl or 3,5-dimethylpyrazolyl ring can be 'frozen out' at low temperatures and two solution rotamers are detected in their NMR spectra. One was assumed to correspond closely to the solid-state crystal structure and the other to a structure in which the five-membered ring had rotated through *ca.* 180° . In the present tmpzt and tdmpzt complexes it is assumed that the pairs of rotamers are again related to each other by near- 180° rotations of the pyrazolyl ring. In the absence of crystal structures, however, their relative orientations with respect to the central triazine ring are not known. It should be noted that these likely non-planar conformations of the ligand (tmpzt) are in contrast to the conformation of free 2,4,6-tris(pyrazol-1-yl)-1,3,5-triazine where X-ray crystallography and electron diffraction results indicate a near-planar geometry.¹²

The activation-energy data suggest that the 1,4-Re–N fluxions proceed far less readily in the tdmpzt than in the tmpzt complexes, the differences in averaged ΔG^\ddagger values being 19.4 kJ mol^{-1} . This compares closely with recent findings⁵ for rhenium complexes of 2,4,6-tris(pyrazol-1-yl)pyrimidines where the average difference in ΔG^\ddagger values for the 4-methylpyrazolyl and 3,5-dimethylpyrazolyl cases was 17.4 kJ mol^{-1} . These large energy differences may be associated with the relative donor strengths of the pyrazolyl N atoms (as measured by estimates of

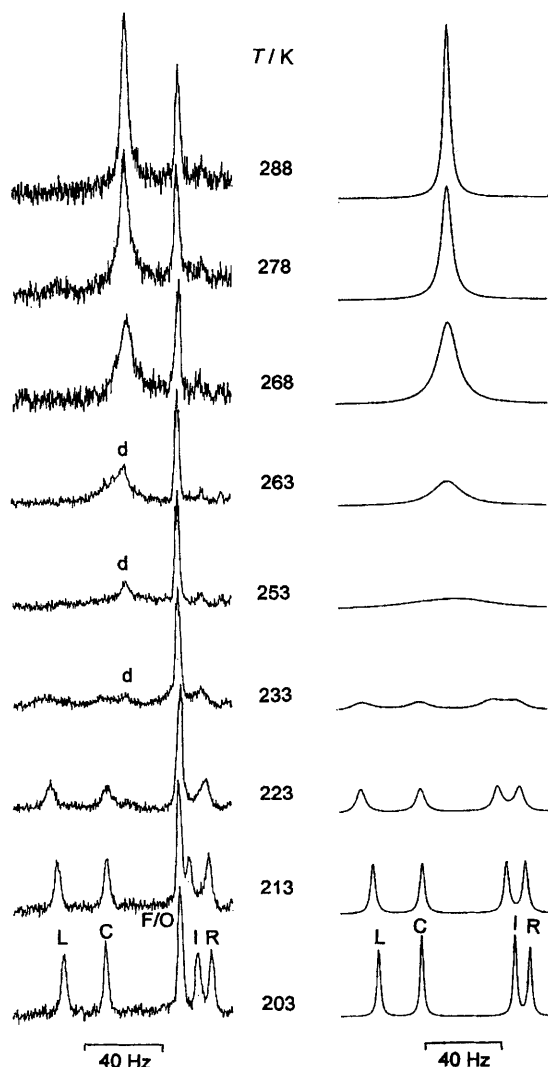


Fig. 3 High-frequency portion of the 300 MHz ^1H NMR spectra of $[\text{ReBr}(\text{CO})_3(\text{tmpzt})]$ at various temperatures showing the effects of the metal-ligand fluxions and 4-methylpyrazolyl ring rotations. Simulated spectra based on best-fit rate constants (Table 7) are shown alongside. d = decomposition signal

Table 8 Hydrogen-1 NMR data * for the complexes $[\{\text{ReX}(\text{CO})_3\}_2(\text{tdmpzt})]$ in CD_2Cl_2 at 303 K

	δ					
X	H_A	H_B	H_C	$\text{H}_\text{D}/\text{H}_\text{D}'$	$\text{H}_\text{E}/\text{H}_\text{E}'$	$\text{H}_\text{F}/\text{H}_\text{F}'$
Br	2.82	6.21	2.59	2.60	6.31	2.52
Cl	2.77	6.15	2.60	2.60	6.27	2.49

* Chemical shifts relative to SiMe_4 (δ 0).

Table 9 Activation-energy data for the fluxional processes in $[\text{ReX}(\text{CO})_3\text{L}]$ complexes

L	X	Rotamer populations (%)	Process ^a	$\Delta H^\ddagger/\text{kJ mol}^{-1}$	$\Delta S^\ddagger/\text{J K}^{-1} \text{mol}^{-1}$	$\Delta G^\ddagger/\text{kJ mol}^{-1}$
tmpzt	Cl	52.0:48.0	FR	50.4 ± 0.15	-1.2 ± 0.6	50.75 ± 0.03
			RR	38.5 ± 0.1	-55.2 ± 0.2	55.0 ± 0.01
	Br	55.0:45.0	FR	50.1 ± 0.1	-2.4 ± 0.3	50.80 ± 0.01
			RR	49.7 ± 0.1	-6.6 ± 0.2	51.67 ± 0.01
	I	55.0:45.0	FR	51.6 ± 0.2	-15.5 ± 3.2	46.98 ± 0.78
			RR	41.0 ± 0.3	-46.2 ± 1.4	54.78 ± 0.07
tdmpzt	Cl	52.7:47.3	F	85.6 ± 2.0	62.9 ± 6.5	66.8 ± 0.1
			RR			42.2^c
	Br	55.0:45.0	F	75.9 ± 3.0	27.1 ± 9.4	67.9 ± 0.2
			RR			41.9^c
	I	56.7:43.3	F	89.7 ± 1.4	59.0 ± 4.1	72.1 ± 0.2
			RR			41.2^d

^a FR = 1,4-Re-N fluxion + rotation; RR = restricted rotation of pyrazolyl ring; F = 1,4-Re-N fluxion. ^b At 298.15 K. ^c For coalescence temperature 203 K. ^d For coalescence temperature 198 K.

the $\text{p}K_a$ values of the respective pro-ligands).³ It should be noted that absolute magnitudes of ΔG^\ddagger values for the 1,4 fluxions are slightly lower for the present complexes than for those based on ligands with a central 1,3-pyrimidine ring.⁵ This must reflect the slightly different donor strengths of the triazine and pyrimidine nitrogens.

The energy barriers for the restricted rotations of the pyrazolyl rings are, surprisingly, higher for the 4-methylpyrazolyl than for the 3,5-dimethylpyrazolyl rings. This is in contrast to the results for the pyrazolylbipyridine complexes $[\text{ReX}(\text{CO})_3\text{L}]$ (L = pbipy or dmpbipy).⁴ Clearly the presence of a heterocyclic N atom rather than a CH moiety in the 5 position of the central ring greatly influences the conformational preferences of the pendant pyrazolyl ring. This is revealed not simply by the magnitudes of the rotation energy barriers but by the relative rotamer populations. For example, in the 3,5-dimethylpyrazolyl complexes $[\text{ReX}(\text{CO})_3(\text{dmpbipy})]$ ⁴ the population ratios are *ca.* 98%:2%, in contrast to 55%:45% in the present $[\text{ReX}(\text{CO})_3(\text{tdmpzt})]$ complexes. It would seem, therefore, to be almost impossible to generalize on the factors governing the rotational characteristics of these pendant pyrazolyl rings.

For the tmpzt complexes where the rotational and fluxional motions occur at comparable rates it was concluded that the preferred pathways for metal fluxions [(iii) in Fig. 1] involve rotations of the two pyrazolyl rings in opposite senses only. This seemingly surprising result simply implies that there is no correlation between the rotations of the two pyrazolyl rings. In other words, it is most probable that the rotations will occur in opposite rather than the same directions. Rates associated with the correlated clockwise or anticlockwise rotations of both rings were very small and considered to be zero within experimental uncertainties.

The NMR evidence for the structures of the dinuclear complexes $[\{\text{ReX}(\text{CO})_3\}_2(\text{tdmpzt})]$ points to a symmetry plane passing through the unco-ordinated N atom of the triazine ring and the C–N bond attaching the unco-ordinated pyrazolyl ring, which is assumed to be undergoing rapid rotation (structure f, Table 8). This structure is closely analogous to the crystal structure of a bis(dicarbonyldichloride)ruthenium complex of 2,4,6-tris(2-pyridyl)-1,3,5-triazine (containing an additional methoxide group).¹³ Such a structure possesses no strong steric

interaction between the rhenium(I) moieties and the pendant 3,5-dimethylpyrazolyl ring, in contrast to the alternative structures of this complex (e and g, Table 8) which could be reached by 1,4-metallotropic shifts of either $\text{ReX}(\text{CO})_3$ moiety. No evidence for these structures was found. Presumably they are disfavoured because of the strong steric interaction of the 5-methyl group of one ring with the closely adjacent equatorial carbonyl group of the rhenium moiety.

Acknowledgements

We thank the Engineering and Physical Sciences Research Council for a postdoctoral research fellowship (to A. G.).

References

- 1 E. W. Abel, K. G. Orrell, A. G. Osborne, H. M. Pain, V. Šik, M. B. Hursthouse and K. M. A. Malik, *J. Chem. Soc., Dalton Trans.*, 1994, 3441 and refs. therein.
- 2 A. Gelling, K. G. Orrell, A. G. Osborne and V. Šik, *J. Chem. Soc., Dalton Trans.*, 1994, 3545.
- 3 E. W. Abel, K. A. Hylands, M. D. Olsen, K. G. Orrell, A. G. Osborne, V. Šik and G. N. Ward, *J. Chem. Soc., Dalton Trans.*, 1994, 1079.
- 4 A. Gelling, K. G. Orrell, A. G. Osborne, V. Šik, M. B. Hursthouse and S. J. Coles, *J. Chem. Soc., Dalton Trans.*, 1996, 203.
- 5 A. Gelling, D. R. Noble, K. G. Orrell, A. G. Osborne and V. Šik, *J. Chem. Soc., Dalton Trans.*, 1996, 3065.
- 6 H. D. Kaesz, R. Bau, D. Hendrickson and J. M. Smith, *J. Am. Chem. Soc.*, 1967, **89**, 2844.
- 7 M. M. Bhatti, Ph.D. Thesis, University of Exeter, 1980.
- 8 D. F. Shriver, *Manipulation of Air-sensitive Compounds*, McGraw-Hill, New York, 1969.
- 9 D. A. Kleier and G. Binsch, DNMR 3 Program 165, Quantum Chemistry Program Exchange, Indiana University, IN, 1970; D. A. Kleier and G. Binsch, *J. Magn. Reson.*, 1970, **3**, 146.
- 10 V. Šik, Ph.D. Thesis, University of Exeter, 1979.
- 11 E. W. Abel, T. P. J. Coston, K. G. Orrell, V. Šik and D. Stephenson, *J. Magn. Reson.*, 1986, **70**, 34.
- 12 A. Echevarria, J. Elguero, A. L. Llamas-Saiz, C. Foces-Foces, G. Schultz and I. Hargittai, *Struct. Chem.*, 1994, **5**, 255.
- 13 N. C. Thomas, B. L. Foley and A. L. Rheingold, *Inorg. Chem.*, 1988, **27**, 3426.

Received 25th April 1996; Paper 6/029011